



HAL
open science

Improved thermoelectric properties in double-filled $\text{Ce}_y\text{Y}_{by}\text{Fe}_{4-x}(\text{CoNi})_x\text{Sb}_{12}$ skutterudites

D. Bérardan, E. Alleno, C. Godart, M. Puyet, Bertrand Lenoir, R. Lackner,
E. Bauer, L. Girard, D. Ravot

► **To cite this version:**

D. Bérardan, E. Alleno, C. Godart, M. Puyet, Bertrand Lenoir, et al.. Improved thermoelectric properties in double-filled $\text{Ce}_y\text{Y}_{by}\text{Fe}_{4-x}(\text{CoNi})_x\text{Sb}_{12}$ skutterudites. *Journal of Applied Physics*, 2005, 98 (3), pp.033710. 10.1063/1.1999854 . hal-03996303

HAL Id: hal-03996303

<https://hal.science/hal-03996303v1>

Submitted on 20 Feb 2023

HAL is a multi-disciplinary open access archive for the deposit and dissemination of scientific research documents, whether they are published or not. The documents may come from teaching and research institutions in France or abroad, or from public or private research centers.

L'archive ouverte pluridisciplinaire **HAL**, est destinée au dépôt et à la diffusion de documents scientifiques de niveau recherche, publiés ou non, émanant des établissements d'enseignement et de recherche français ou étrangers, des laboratoires publics ou privés.

Improved thermoelectric properties in double-filled $\text{Ce}_{1-x}\text{Y}_x\text{Sb}_{12}$ skutterudites

D. Bérardan, E. Alleno, C. Godart, M. Puyet, B. Lenoir et al.

Citation: *J. Appl. Phys.* **98**, 033710 (2005); doi: 10.1063/1.1999854

View online: <http://dx.doi.org/10.1063/1.1999854>

View Table of Contents: <http://jap.aip.org/resource/1/JAPIAU/v98/i3>

Published by the [American Institute of Physics](#).

Additional information on *J. Appl. Phys.*

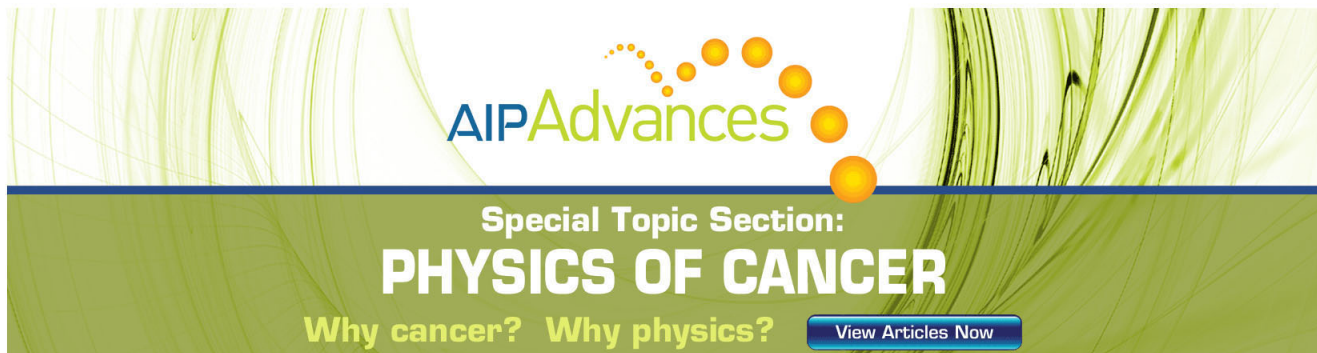
Journal Homepage: <http://jap.aip.org/>

Journal Information: http://jap.aip.org/about/about_the_journal

Top downloads: http://jap.aip.org/features/most_downloaded

Information for Authors: <http://jap.aip.org/authors>

ADVERTISEMENT



AIP Advances

Special Topic Section:
PHYSICS OF CANCER

Why cancer? Why physics? [View Articles Now](#)

Improved thermoelectric properties in double-filled $\text{Ce}_{y/2}\text{Yb}_{y/2}\text{Fe}_{4-x}(\text{Co/Ni})_x\text{Sb}_{12}$ skutterudites

D. Bérardan, E. Alleno,^{a)} and C. Godart

Laboratoire de Chimie Métallurgique des Terres-Rares, Unité Propre de Recherche (UPR) 209, Institut des Sciences Chimiques Seine-Amont (ISCSA), Centre National de la Recherche Scientifique (CNRS), 2-8 rue Henri Dunant, 94320 Thiais Cedex, France

M. Puyet and B. Lenoir

Laboratoire de Physique des Matériaux, Unité Mixte de Recherche (UMR) 7556, Ecole Nationale Supérieure de Mines de Nancy (ENSMN), Parc de Saurupt, 54042 Nancy Cedex, France

R. Lackner and E. Bauer

Institute of Solid State Physics, Vienna University of Technology, A-1040 Wien, Austria

L. Girard and D. Ravot

Laboratoire de Physico-Chimie de la Matière Condensée, Unité Mixte de Recherche (UMR) 5617, Université de Montpellier II, 34095 Montpellier Cedex 5, France

(Received 4 February 2005; accepted 16 June 2005; published online 9 August 2005)

We have investigated the thermal and electrical properties of filled skutterudites belonging to the series $\text{Ce}_{1-z}\text{Yb}_z\text{Fe}_4\text{Sb}_{12}$ and $\text{Ce}_{y/2}\text{Yb}_{y/2}\text{Fe}_{4-x}(\text{Co/Ni})_x\text{Sb}_{12}$, as well as their potential for thermoelectric power generation. In the first series, increasing the Yb fraction decreases the resistivity and thermopower. These effects are related to the variations of valence of Yb with the Yb fraction (from 2.2 in $\text{Yb}_{0.92}\text{Fe}_4\text{Sb}_{12}$ to 2.7 in $\text{Ce}_{0.85}\text{Yb}_{0.05}\text{Fe}_4\text{Sb}_{12}$). The power factor is increased in $\text{Ce}_{0.40}\text{Yb}_{0.53}\text{Fe}_4\text{Sb}_{12}$ while the thermal conductivity is reduced and this leads to an improved figure of merit in this compound when compared to $\text{Ce}_{0.85}\text{Fe}_4\text{Sb}_{12}$. Co or Ni substitution was used to tune the carrier concentration and improve the power factor: we measure a $ZT=0.5$ at 500 K in $\text{Ce}_{0.44}\text{Yb}_{0.32}\text{Fe}_{3.02}\text{Co}_{0.98}\text{Sb}_{12}$ and an extrapolation leads to $ZT=0.95$ at 800 K, which is close to state-of-the-art $\text{Ce}_{0.28}\text{Fe}_{1.52}\text{Co}_{2.48}\text{Sb}_{12}$ although the composition is far from being optimized. Double filling happens to be a promising path to provide good thermoelectric performances. © 2005 American Institute of Physics. [DOI: 10.1063/1.1999854]

INTRODUCTION

The skutterudite family has been extensively studied in the past few years because of its very promising properties for high-temperature thermoelectric applications.^{1,2} The efficiency of a thermoelectric material used for power generation or cooling applications is usually characterized by the dimensionless thermoelectric figure of merit ZT defined as $ZT = \sigma S^2 T / \lambda = \sigma S^2 T / (\lambda_e + \lambda_L)$, where σ , S , and λ are the electrical conductivity, Seebeck coefficient or thermopower, and total thermal conductivity, respectively. λ_e and λ_L are the electronic and lattice parts of the thermal conductivity. λ_e and σ are related by the Wiedemann-Franz law $\lambda_e = L_0 T \sigma$ valid for metals, with the Lorentz number $L_0 = 2.44 \times 10^{-8} \text{ W } \Omega \text{ K}^{-2}$. The energy conversion efficiency increases when increasing ZT . Therefore, the requirements for an optimum thermoelectric material will be to conduct heat like a glass (low λ_L) and the electrons like a crystal (high σ) rendering the phonon glass and electron crystal (PGEC) concept.³

Binary skutterudites crystallize in a body-centered-cubic (bcc) structure with space group $Im\bar{3}$ (Ref. 4) and have a general formula MX_3 ($M = \text{Co, Rh, or Ir}$ and $X = \text{P, As, or Sb}$)

(Ref. 5) with M occupying the $8c$ positions $(\frac{1}{4}, \frac{1}{4}, \frac{1}{4})$ of the crystallographic structure and X the $24g$ positions $(0, y, z)$. They are small band-gap semiconductors with high thermopower and high charge-carrier mobilities.² However, their dimensionless figures of merit ZT remain too low for thermoelectric applications because of their high lattice thermal conductivities (the room-temperature lattice thermal conductivity is about ten times higher in CoSb_3 than in state-of-the-art Bi_2Te_3 -based alloys^{6,7}). An effective way to reduce the lattice thermal conductivity of the skutterudites and to make them viable for thermoelectric applications is to fill the large icosahedral void in the $2a$ site $(0, 0, 0)$ of the crystallographic structure with an electropositive element to form filled skutterudites with general formula RM_4X_{12} ($R = \text{electropositive element, } M = \text{Fe, Ru, or Os}$). Many electropositive elements have been explored to optimize ZT , including most of the rare earths,² Ba,⁸ Tl,⁹ and Sn.¹⁰ The lattice thermal conductivity of filled skutterudites is strongly reduced as compared to that of binary skutterudites.¹ This decrease originates from the possibility for the filler atom to “rattle” around its equilibrium position in the oversized cage and thus to effectively scatter the heat conducting phonons.¹¹ Since CoSb_3 is a semiconductor, a simple electron count shows that RM_4X_{12} ($M = \text{Fe, Ru, or Os}$) should be metallic with a divalent or trivalent filler atom. This is effectively

^{a)}Electronic mail: eric.alleno@glvt-cnrs.fr

observed¹² and the thermopower is strongly reduced in RM_4X_{12} ($M=Fe, Ru, \text{ or } Os$): for instance, the room-temperature thermopower is $\sim 75 \mu\text{V K}^{-1}$ in $\text{CeFe}_4\text{Sb}_{12}$ (Ref. 12) as compared to $\sim 230 \mu\text{V K}^{-1}$ in nonintentionally doped CoSb_3 .⁶ To restore the semiconducting behavior and the high power factor ($S^2\sigma$ is maximum at around 10^{19} carriers/cm³), it is necessary to reduce the carrier concentration $[p]$ by substituting Co ($3d^7$) or Ni ($3d^8$) for Fe ($3d^6$) on the M site of the structure. However the R atom filling rate decreases as the iron fraction decreases,^{13,14} which leads to partially filled skutterudites with general formula $R_yM_{4-y}M'_y\text{Sb}_{12}$ (Ref. 15) ($y < 1$). The lattice thermal conductivity is strongly reduced in partially filled skutterudites as compared to the fully filled ones, with a minimum close to $y \sim 0.6$.¹⁵ This is related to a scattering of the heat conducting phonons by mass fluctuations on the R site (due to mass differences between the filler atom and a vacancy).¹⁶ In state-of-the-art skutterudites, a dimensionless figure of merit $ZT = 1.25$ has been obtained at 900 K for n -type $\text{Ba}_{0.3}\text{Ni}_{0.05}\text{Co}_{3.95}\text{Sb}_{12}$,¹⁷ and $ZT = 1.1$ has been obtained at 750 K for p -type $\text{Ce}_{0.28}\text{Co}_{2.48}\text{Fe}_{1.52}\text{Sb}_{12}$.¹⁸ However, even in this compounds the lattice thermal conductivity remains quite high and could lead to further improvements. It has been shown recently in $R_y\text{Co}_4\text{Sb}_{12}$ that multifilling is an effective approach to generate additional phonon scattering and thus to decrease the lattice thermal conductivity.¹⁹ Furthermore, this reduction is more pronounced when the valence states of the two filler atoms are different.¹⁹

Recently, we have shown the possibility of mixing cerium and ytterbium on the $2a$ site of the structure to form a complete solid solution $\text{Ce}_{1-y}\text{Yb}_y\text{Fe}_4\text{Sb}_{12}$,²⁰ and of tuning the carrier concentration by substituting Co or Ni for Fe to form partially filled skutterudites with general formula $\text{Ce}_{y/2}\text{Yb}_{y/2}\text{Fe}_{4-x}(\text{Co/Ni})_x\text{Sb}_{12}$.²¹ We have shown that Ce is always in a trivalent state, whereas Yb is in a mixed valence state that depends on the Yb fraction.²² This paper presents the thermal and electrical transport properties of these series from 4 to 800 K. The effect of double filling on the thermoelectric properties is analyzed. Finally, the potential of double-filled skutterudites with respect to the thermoelectric performance as well as possible improvements are discussed.

EXPERIMENT

All samples described in this study were prepared by standard arc melting on a water-cooled copper hearth under Ar atmosphere and subsequent annealing as described in Ref. 22. For thermal and electrical conductivity measurements, densification of the samples was achieved by uniaxial hot pressing in graphite dies under an argon atmosphere to avoid antimony losses at 600 °C and under a pressure of 50 MPa for 2 h. For thermopower measurements, densification was achieved by pressing at 300 °C under 400 MPa with a PO Weber hot press tool model 10HS.

Structural and chemical characterizations of the samples were performed by x-ray diffraction (XRD) and electron probe microanalysis (EPMA) as described in Ref. 22. All the compositions reported in this article are final compositions measured by EPMA and normalized to full occupancy of the

transition-metal site. The antimony fraction has been fixed to full occupancy, as the observed deviation is not significant. XRD and EPMA show that every sample is constituted by one single skutterudite phase and faint amounts of Sb, $\text{Fe}_{1-x}(\text{Co/Ni})_x\text{Sb}_2$, and/or $\text{Ce}_{1-z}\text{Yb}_z\text{Sb}_2$. All samples contain more than 95% of the skutterudite phase. No broadening or shift of the Bragg peaks can be observed, thus revealing that the skutterudite phases are well crystallized and homogeneous.

For electrical conductivity and thermopower, all samples were measured in a direction perpendicular to the pressing direction. Thermopower measurements were made on $10 \times 2 \times 1\text{-mm}^3$ samples between 120 and 300 K using a homemade apparatus with Chromel/AuFe or Chromel/Constantan thermocouples, as described in Ref. 22, with a constant thermal gradient $\Delta T = 1$ K. The measurements between 300 and 520 K were performed on another homemade system. While the sample is kept at one temperature (T_c) in a furnace, a hot point (T_h) comes shortly in contact with the sample. For each temperature T_c we use several T_h to get different gradients ΔT (from 20 to 200 K). The thermopower is the slope at each temperature of the linear dependence of ΔV vs ΔT . Because of the use of two different experimental setups to measure thermopower, a small mismatch between the data taken at low temperature and those obtained at high temperature arises (see Fig. 5). The agreement between the two data sets remains within 15% at room temperature and moreover, we observed that the overall trend is preserved. Electrical resistivity measurements were made on square-shape samples ($4 \times 4 \times 0.5 \text{ mm}^3$) between 300 and 800 K using a standard Van der Paw method and between 4 and 300 K using a Quantum Design physical property measurement system (PPMS) in ac mode. Hall-effect measurements were performed on the same samples as electrical resistivity between 4 and 300 K and up to 7 T using a Quantum Design PPMS. The Hall coefficient was deduced from the slope of the Hall resistivity versus field curves, $\rho_H(H)$. The carrier concentration (n or p) was calculated from the Hall coefficient R_H , assuming a single-carrier model and a Hall factor of unity. Hall mobility μ_H was obtained using $\mu_H = |1/\rho n e|$ with ρ the electrical resistivity. Above room temperature, thermal conductivity was determined by measuring the thermal diffusivity on a 12-mm-diameter disc by a laser flash technique and the specific heat by differential scanning calorimetry. Thermal-conductivity measurements below room temperature were performed in a flow cryostat on rectangular parallelpiped samples (length: about 1 cm and cross section: about $2\text{--}3 \text{ mm}^2$), which were kept cold by anchoring one end of the sample onto a thick copper panel mounted on the heat exchanger of the cryostat. The temperature difference along the sample, established by electrical heating, was determined by means of a differential thermocouple (Au + 0.07% Fe/Chromel). The measurement was performed under high vacuum and three shields mounted around the sample reduced the heat losses due to radiation at finite temperatures. The innermost of these shields is kept on the temperature of the sample via an extra heater powered by a second temperature controller.

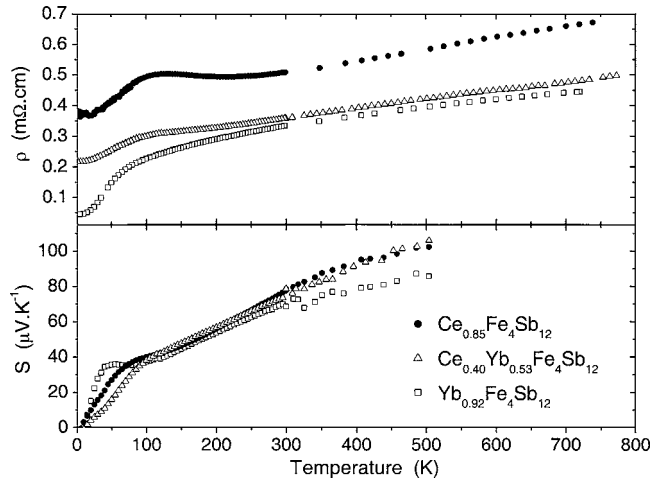


FIG. 1. Temperature dependence of the electrical resistivity (top) and of the thermopower (bottom) in $Ce_{1-z}Yb_zFe_4Sb_{12}$.

RESULTS AND DISCUSSION

Figure 1 shows the temperature dependences of the thermopower (bottom) and of the electrical resistivity (top) for three samples belonging to the series $Ce_{1-z}Yb_zFe_4Sb_{12}$. As expected from a simple electron count, all samples appear p type, as can be deduced from the positive values of the thermopower. For all samples, the thermopower grows continuously up to 520 K (limit of our measurement setup). For samples with $z=0$ and $z \sim 1$, its magnitude is consistent with the results reported by Sales for $CeFe_4Sb_{12}$ (Ref. 1) and by Anno *et al.* for $YbFe_4Sb_{12}$.²³ This last compound also exhibits a hump in $S(T)$ around 50 K, which was previously observed and was described as a Kondo coherence peak²⁴ originating from the Yb $4f$ heavy electrons.²⁵ However, this interpretation is questionable since we showed that the valence of Yb is close to 2 (Ref. 20) and that paramagnetism is dominated by the $[Fe_4Sb_{12}]$ subunit. More recently, this 50-K hump was also observed in $S(T)$ for AFe_4Sb_{12} with A = divalent and nonmagnetic Ca, Sr, and Ba (Ref. 26) and attributed to the saturation of the contribution from Fe $3d$ spin fluctuations above a characteristic temperature $T_{sf} \sim 50$ K. Although a phonon drag contribution cannot be formally excluded, we agree with this last interpretation. Except in the low-temperature part (under about 100 K) where magnetism contributes, the thermopower of the mixed compound $Ce_{0.40}Yb_{0.53}Fe_4Sb_{12}$ lies between that of $YbFe_4Sb_{12}$ and $CeFe_4Sb_{12}$. This result is consistent with Hall-effect measurements reported in Table I, which shows that the concentration of holes increases when the ytterbium fraction increases. This behavior is related to the variation of the

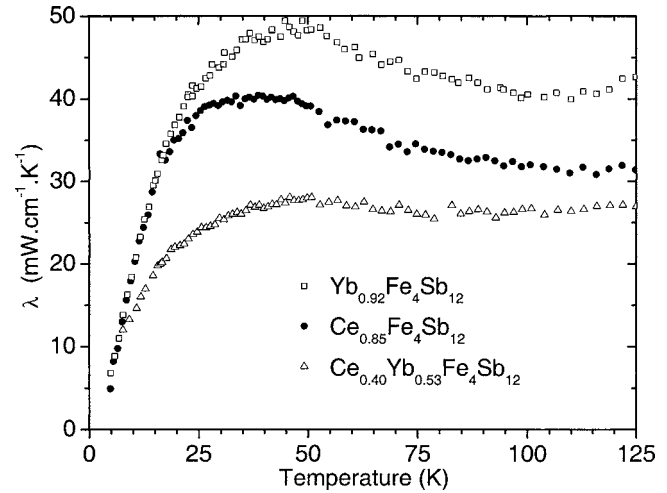


FIG. 2. Temperature dependence of the thermal conductivity in $Ce_{1-z}Yb_zFe_4Sb_{12}$.

valence of the rare earth; whereas Ce is always trivalent, the Yb valence state decreases from 2.7 in $Ce_{0.85}Yb_{0.05}Fe_4Sb_{12}$ to 2.2 in $Yb_{0.92}Fe_4Sb_{12}$.²⁰ The electrical resistivity increases with increasing temperature for all samples belonging to the $Ce_{1-z}Yb_zFe_4Sb_{12}$ series as can be expected for semimetals. The high temperature values measured for $Yb_{0.92}Fe_4Sb_{12}$ and $Ce_{0.85}Fe_4Sb_{12}$ are slightly lower than those reported in the literature,^{27,28} thus revealing a very good densification of our samples. The resistivity of $Ce_{0.40}Yb_{0.53}Fe_4Sb_{12}$ lies between that of $Yb_{0.92}Fe_4Sb_{12}$ and $Ce_{0.85}Fe_4Sb_{12}$, in agreement with the dependence of the thermopower with substitution. The hole mobility decreases with increasing carrier concentration (see Table I), as it has been observed in the series $Yb_yFe_{4-x}Ni_xSb_{12}$ (Ref. 23) where this behavior has been attributed to an increase of the effective mass with increasing carrier concentration.²³ However, this decrease of μ does not dominate the increase of $[p]$ and the decrease in ρ .

Figure 2 shows the low-temperature dependence of the thermal conductivity in the series $Ce_{1-z}Yb_zFe_4Sb_{12}$. The thermal conductivity of $Yb_{0.92}Fe_4Sb_{12}$ is higher than that of $Ce_{0.85}Fe_4Sb_{12}$. This is related to an increase of the electronic part of the thermal conductivity λ_e with increasing Yb fraction. However, although the electrical resistivity of $Ce_{0.40}Yb_{0.53}Fe_4Sb_{12}$ is lower than that of $Ce_{0.85}Fe_4Sb_{12}$, its thermal conductivity is lower, too. Therefore, the double filling of the cage with two filler atoms of different valence states appears to be an effective path to reduce the thermal conductivity, as was first shown by Chen in $(R-R')_yCo_4Sb_{12}$.¹⁹ The thermal conductivity is almost constant from room temperature up to 825 K in $Ce_{0.40}Yb_{0.53}Fe_4Sb_{12}$ (not shown).

TABLE I. Room-temperature thermopower S , electrical resistivity ρ , carrier concentration $[p]$, carrier mobility μ_H , and ZT values in $Ce_{1-z}Yb_zFe_4Sb_{12}$. Thermal conductivity λ at 150 K.

	S ($\mu V K^{-1}$)	ρ (Ωcm)	$[p]$ (cm^{-3})	μ_H ($cm^2 V^{-1} s^{-1}$)	λ ($mW cm^{-1} K^{-1}$)	ZT
$Ce_{0.85}Fe_4Sb_{12}$	78.1	483×10^{-6}	1.0×10^{21}	11.5	31.1	0.12
$Ce_{0.40}Yb_{0.53}Fe_4Sb_{12}$	73.4	388×10^{-6}	3.0×10^{21}	5.5	28.3	0.14
$Yb_{0.92}Fe_4Sb_{12}$	68.4	333×10^{-6}	5.0×10^{21}	3.5	40.5	0.10

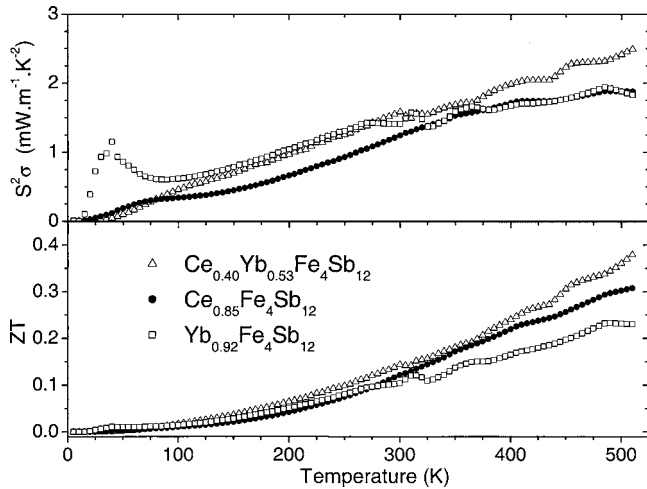


FIG. 3. Temperature dependence of the power factor (top) and of the dimensionless thermoelectric figure of merit (bottom) in $Ce_{1-z}Yb_zFe_4Sb_{12}$. ZT data for $Ce_{0.85}Fe_4Sb_{12}$ and $Yb_{0.92}Fe_4Sb_{12}$ have been extrapolated from low-temperature thermal-conductivity measurements.

Figure 3 shows the temperature dependence of the power factor $S^2\sigma$ (top) and of the dimensionless thermoelectric figure of merit (bottom). ZT data for $Ce_{0.85}Fe_4Sb_{12}$ and $Yb_{0.92}Fe_4Sb_{12}$ have been extrapolated from low-temperature thermal-conductivity measurements. At 520 K, the power factor is close in $Yb_{0.92}Fe_4Sb_{12}$ and $Ce_{0.85}Fe_4Sb_{12}$: the electrical resistivity is lower in the former one and the thermopower is higher in the last one, thus resulting in similar power factor. However, it is clearly enhanced in the double-filled compound $Ce_{0.40}Yb_{0.53}Fe_4Sb_{12}$. Moreover, as can be seen in Fig. 3, the figure of merit ZT is enhanced in $Ce_{0.40}Yb_{0.53}Fe_4Sb_{12}$ by more than 20% as compared to $Ce_{0.85}Fe_4Sb_{12}$ and by more than 60% as compared to $Yb_{0.92}Fe_4Sb_{12}$. Therefore, double-filled skutterudites seems to be of significant interest to improve the power generation efficiency.

To reach higher ZT values, it is mandatory to tune the charge-carrier concentration. This can be achieved by substituting Co or Ni for Fe on the metal site. Figure 4 shows

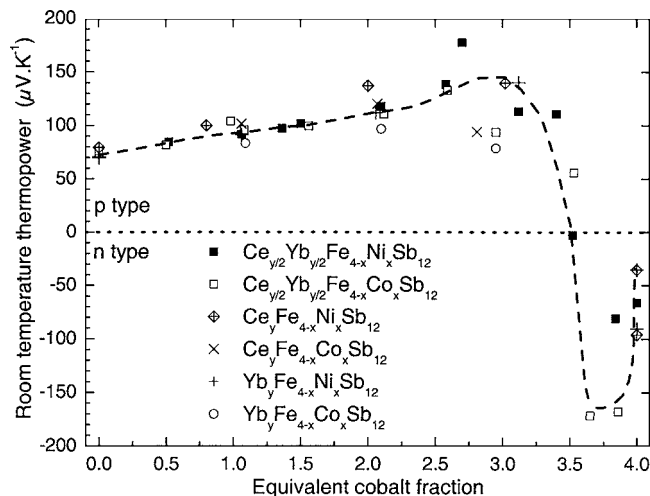


FIG. 4. Room-temperature thermopower in the series $(Ce-Yb)_yFe_{4-x}(Co/Ni)_xSb_{12}$ vs equivalent cobalt fraction as described in text. The dashed line is a guide for the eyes.

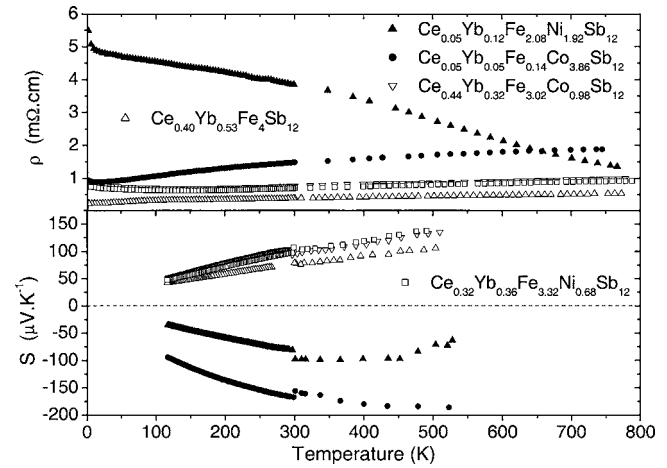


FIG. 5. Temperature dependence of the electrical resistivity (top) and of the thermopower (bottom) in $Ce_{y/2}Yb_{y/2}Fe_{4-x}(Co/Ni)_xSb_{12}$.

the room-temperature thermopower in the series $(Ce-Yb)_yFe_{4-x}(Co/Ni)_xSb_{12}$ as a function of the equivalent cobalt fraction defined in Ref. 14. It is considered from a simple electron count that the substitution of one iron atom by one nickel atom is equivalent to the substitution of two iron atoms by two cobalt atoms. This enables us to directly compare the results obtained for the Fe–Ni and the Fe–Co series. Figure 4 shows a crossover from p - to n -type conductivity for an equivalent cobalt fraction of about 3.5, which can be easily explained by a simple carrier count: the Fe–Co or Fe–Ni substitution reduces the holes' concentration which is eventually overcompensated by the electrons provided by the filler atom(s) for rich Co or Ni skutterudites. This simple count also explains the increase of S before the p - n transition. The thermopower reaches its highest absolute values close to the p - n transition, and its magnitude very weakly depends on the nature of the filler atom.

The thermal dependence of the thermopower and of the electrical resistivity are shown in Fig. 5 for some samples belonging to the series $Ce_{y/2}Yb_{y/2}Fe_{4-x}(Co/Ni)_xSb_{12}$. As can be deduced from Fig. 4, iron-rich samples appear p type, whereas cobalt-rich or nickel-rich samples appear n type. Similar to the series $Ce_{1-z}Yb_zFe_4Sb_{12}$, the absolute value of the thermopower grows continuously up to 520 K and no evidence of a maximum can be observed, except for $Ce_{0.05}Yb_{0.12}Fe_{2.08}Ni_{1.92}Sb_{12}$ whose thermopower decreases at high temperature. The latter is probably related to the semi-conducting nature of this compound (see top of Fig. 5). All the other samples are semimetals with low resistivity values, which increase with increasing temperature. These values are similar to those reported in the literature for skutterudites with similar cobalt or iron fraction [see, for example (Refs. 23 and 29)].

Figure 6 shows the low-temperature dependence of the thermal conductivity. The thermal conductivity first decreases when substituting cobalt or nickel for iron to form partially filled skutterudites, and then increases when the rare-earth concentration further decreases. This behavior is consistent with the “mass fluctuation scattering” model proposed by Meisner *et al.*,¹⁵ which showed that the minimum thermal conductivity in $Ce_yFe_{4-x}Co_xSb_{12}$ occurs for $y \sim 2/3$.

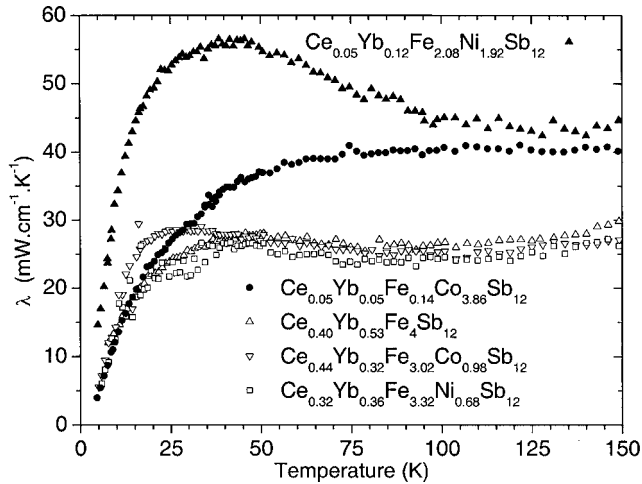


FIG. 6. Temperature dependence of the thermal conductivity in $\text{Ce}_{y/2}\text{Yb}_{y/2}\text{Fe}_{4-x}(\text{Co/Ni})_x\text{Sb}_{12}$.

The thermal conductivity is almost constant from room temperature up to 825 K in $\text{Ce}_{0.44}\text{Yb}_{0.32}\text{Fe}_{3.02}\text{Co}_{0.98}\text{Sb}_{12}$ (not shown).

The temperature dependences of the power factor $S^2\sigma$ and of the thermoelectric figure of merit are shown in Fig. 7. Whereas the power factor and ZT are similar in p -type $\text{Ce}_{0.44}\text{Yb}_{0.32}\text{Fe}_{3.02}\text{Co}_{0.98}\text{Sb}_{12}$ and $\text{Ce}_{0.32}\text{Yb}_{0.36}\text{Fe}_{3.32}\text{Ni}_{0.68}\text{Sb}_{12}$, with similar equivalent cobalt fraction, this is not the case in n -type $\text{Ce}_{0.05}\text{Yb}_{0.12}\text{Fe}_{2.08}\text{Ni}_{1.92}\text{Sb}_{12}$ and $\text{Ce}_{0.05}\text{Yb}_{0.05}\text{Fe}_{0.14}\text{Co}_{3.86}\text{Sb}_{12}$. They are strongly degraded in the Ni-based n -type skutterudite. While the hole concentration and mobility are similar in iron-rich Ni-based and Co-based skutterudites, the electron concentration and mobility are very different in iron-poor skutterudites (see Table II). Especially, the mobility is strongly decreased in the Ni-rich skutterudite as compared to the Co-rich ones. Several mechanisms could explain this behavior. This decrease could be related to the theoretical calculations performed by Lassalle *et al.*³⁰ on $\text{Fe}_2\text{Ni}_2\text{Sb}_{12}$, which shows that the disorder induced by the random distribution of iron and nickel atoms has a strong effect on the position and charge of antimony atoms, and therefore on the band structure and on the effective mass. This could also be related to the huge structural disorder induced by the substitution of iron by nickel; whereas less than 4% of the cobalt atoms are substituted by iron in $\text{Ce}_{0.05}\text{Yb}_{0.05}\text{Fe}_{0.14}\text{Co}_{3.86}\text{Sb}_{12}$, almost 50% of the iron atoms are substituted by nickel in $\text{Ce}_{0.05}\text{Yb}_{0.12}\text{Fe}_{2.08}\text{Ni}_{1.92}\text{Sb}_{12}$. Nevertheless, it appears in our case that cobalt substitutions are more relevant than nickel substitutions to achieve good thermoelectric properties. The best figure of merit is observed in

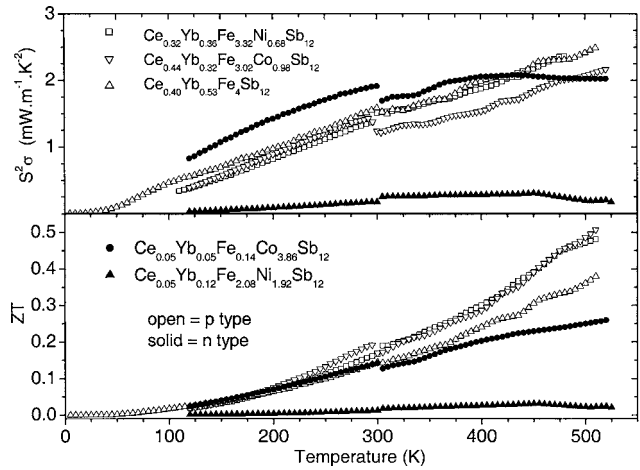


FIG. 7. Temperature dependence of the power factor (top) and of the thermoelectric figure of merit (bottom) in $\text{Ce}_{y/2}\text{Yb}_{y/2}\text{Fe}_{4-x}(\text{Co/Ni})_x\text{Sb}_{12}$. ZT data for $\text{Ce}_{0.32}\text{Yb}_{0.36}\text{Fe}_{3.32}\text{Ni}_{0.68}\text{Sb}_{12}$, $\text{Ce}_{0.05}\text{Yb}_{0.05}\text{Fe}_{0.14}\text{Co}_{3.86}\text{Sb}_{12}$, and $\text{Ce}_{0.05}\text{Yb}_{0.12}\text{Fe}_{2.08}\text{Ni}_{1.92}\text{Sb}_{12}$ have been extrapolated from low-temperature thermal-conductivity measurements.

$\text{Ce}_{0.44}\text{Yb}_{0.32}\text{Fe}_{3.02}\text{Co}_{0.98}\text{Sb}_{12}$ with $ZT=0.55$ at 525 K. However, one must keep in mind that this composition has not been optimized and that important enhancements are certainly possible with higher cobalt fractions.

Figure 8 shows the figure of merit of $\text{Ce}_{0.44}\text{Yb}_{0.32}\text{Fe}_{3.02}\text{Co}_{0.98}\text{Sb}_{12}$ up to 800 K. Thermopower has been extrapolated above 550 K in this compound by assuming rates of variation similar to what Tang *et al.* found between 500 and 800 K in $\text{CeFe}_{4-x}\text{Co}_x\text{Sb}_{12}$ with a similar cobalt fraction ($x=1.02$):¹⁸ $+0.15 \mu\text{V K}^{-2}$ from 500 to 700 K and $-0.08 \mu\text{V K}^{-2}$ above 700 K. This assumption is reasonable because we have observed in literature that the high-temperature thermal variations of thermopower in $(\text{Ce or Yb})_y\text{Fe}_{4-x}(\text{Co or Ni})_x\text{Sb}_{12}$ compounds depend mainly on the cobalt or nickel fraction.^{18,23} We have also plotted the figure of merit of $\text{Ce}_{0.74}\text{Fe}_{2.98}\text{Co}_{1.02}\text{Sb}_{12}$ (same cobalt fraction) and $\text{Ce}_{0.28}\text{Fe}_{1.52}\text{Co}_{2.48}\text{Sb}_{12}$ (state of the art) published by Tang *et al.*¹⁸ for comparison. For a similar cobalt fraction, the figure of merit is strongly enhanced in the double-filled skutterudite: it increases from $ZT=0.4$ at 700 K in $\text{Ce}_{0.74}\text{Fe}_{2.98}\text{Co}_{1.02}\text{Sb}_{12}$ to $ZT=0.85$ at 700 K in $\text{Ce}_{0.44}\text{Yb}_{0.32}\text{Fe}_{3.02}\text{Co}_{0.98}\text{Sb}_{12}$. The latter exhibits a figure of merit very close to that of state-of-the-art $\text{Ce}_{0.28}\text{Fe}_{1.52}\text{Co}_{2.48}\text{Sb}_{12}$, although the composition has not been optimized. From this result, high ZT values are expected in double-filled skutterudites, probably significantly higher than $ZT=1$.

TABLE II. Room-temperature thermopower S , electrical resistivity ρ , carrier concentration $[p]$ or $[n]$, carrier mobility μ_H , and ZT values in $\text{Ce}_{y/2}\text{Yb}_{y/2}\text{Fe}_{4-x}(\text{Co/Ni})_x\text{Sb}_{12}$. Thermal conductivity λ at 150 K.

	S ($\mu\text{V K}^{-1}$)	ρ ($\Omega \text{ cm}$)	$[n/p]$ (cm^{-3})	μ_H ($\text{cm}^2 \text{ V}^{-1} \text{ s}^{-1}$)	λ ($\text{mW cm}^{-1} \text{ K}^{-1}$)	ZT
$\text{Ce}_{0.44}\text{Yb}_{0.32}\text{Fe}_{3.02}\text{Co}_{0.98}\text{Sb}_{12}$	103.7	754×10^{-6}	2.4×10^{21}	3.5	24.5	0.19
$\text{Ce}_{0.32}\text{Yb}_{0.36}\text{Fe}_{3.32}\text{Ni}_{0.68}\text{Sb}_{12}$	97.7	691×10^{-6}	3.0×10^{21}	3	25	0.17
$\text{Ce}_{0.05}\text{Yb}_{0.05}\text{Fe}_{0.14}\text{Co}_{3.86}\text{Sb}_{12}$	-168.1	1480×10^{-6}	1.7×10^{20}	27	40.5	0.14
$\text{Ce}_{0.05}\text{Yb}_{0.12}\text{Fe}_{2.08}\text{Ni}_{1.92}\text{Sb}_{12}$	-81.4	3820×10^{-6}	6.0×10^{20}	3	43.5	0.01

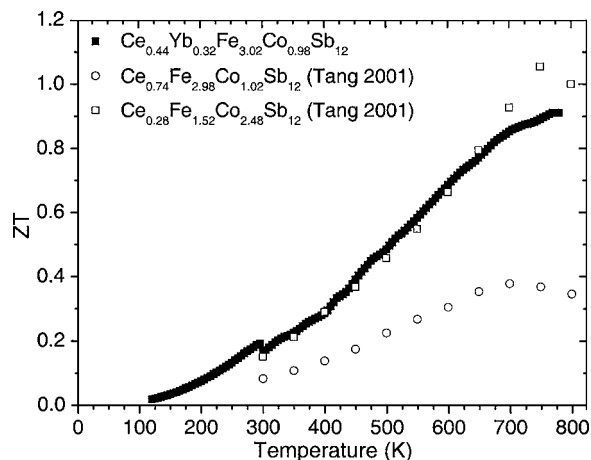


FIG. 8. Temperature dependence of ZT in $\text{Ce}_{0.44}\text{Yb}_{0.32}\text{Fe}_{3.02}\text{Co}_{0.98}\text{Sb}_{12}$. Thermopower has been extrapolated above 550 K.

CONCLUSION

We have studied the thermoelectric properties of skutterudites belonging to the series $\text{Ce}_{y/2}\text{Yb}_{y/2}\text{Fe}_{4-x}(\text{Co}/\text{Ni})_x\text{Sb}_{12}$, where Ce is trivalent, whereas the Yb valence decreases when the Yb fraction increases. The power factor and the thermoelectric figure of merit are clearly enhanced in $\text{Ce}_{0.40}\text{Yb}_{0.53}\text{Fe}_4\text{Sb}_{12}$ as compared to $\text{Ce}_{0.85}\text{Fe}_4\text{Sb}_{12}$ and $\text{Yb}_{0.92}\text{Fe}_4\text{Sb}_{12}$. The carrier concentration can be tuned by substituting Co or Ni on the Fe site, which also diminishes the thermal conductivity. It has been shown that the cobalt substitution is more effective than the nickel substitution to achieve high power factor or figure of merit in n -type samples. $ZT=0.5$ has been observed at 500 K in $\text{Ce}_{0.44}\text{Yb}_{0.32}\text{Fe}_{3.02}\text{Co}_{0.98}\text{Sb}_{12}$ and an extrapolation leads to $ZT=0.95$ at 800 K, which is close to state-of-the-art $\text{Ce}_{0.28}\text{Fe}_{1.52}\text{Co}_{2.48}\text{Sb}_{12}$ although the composition is far from being optimized. Therefore, double-filled Ce+Yb skutterudites appear to be very promising with respect to thermoelectricity, and ZT values significantly above unity could possibly be reached.

ACKNOWLEDGMENTS

We acknowledge E. Leroy for microprobe measurements, O. Rouleau for thermopower measurements, and the Franco-Austrian exchange program Amadeus 05545RE. Parts of the work were performed under the auspices of the Austrian FWF P16370.

- ¹B. C. Sales, D. Mandrus, and R. K. Williams, *Science* **272**, 1325 (1996).
- ²C. Uher, Proceedings of the 21st International Conference on Thermoelectrics, Long Beach, California, USA, 25–29 August 2002 (IEEE, Piscataway), p. 35.
- ³G. A. Slack, in *Thermoelectric Handbook*, edited by D. M. Rowe (Chemical Rubber, Boca Raton, FL, 1995), p. 407.
- ⁴I. Z. Otfedal, *Z. Kristallogr.* **66**, 517 (1928).
- ⁵A. Kjekshus and T. Rakke, *Acta Chem. Scand., Ser. A* **28**, 99 (1974).
- ⁶D. T. Morelli, T. Caillat, J. P. Fleurial, A. Borshchevsky, J. W. Vanderlande, B. Chen, and C. Uher, *Phys. Rev. B* **51**, 9622 (1995).
- ⁷C. B. Satterthwaite and R. W. Ure, *Phys. Rev.* **108**, 1164 (1957).
- ⁸X. F. Tang, L. D. Chen, T. Goto, T. Hirai, and R. Z. Yuan, *J. Mater. Res.* **17**, 2953 (2002).
- ⁹B. C. Sales, B. C. Chakoumakos, and D. Mandrus, *Phys. Rev. B* **61**, 2475 (2000).
- ¹⁰G. S. Nolas, H. Takizawa, T. Endo, H. Sellin, and D. C. Johnson, *Appl. Phys. Lett.* **77**, 52 (2000).
- ¹¹G. S. Nolas, G. A. Slack, D. T. Morelli, T. M. Tritt, and A. C. Ehrlich, *J. Appl. Phys.* **79**, 4002 (1996).
- ¹²D. T. Morelli and G. P. Meisner, *J. Appl. Phys.* **77**, 3777 (1995).
- ¹³B. Chen, J. H. Xu, C. Uher, D. T. Morelli, G. P. Meisner, J. P. Fleurial, T. Caillat, and A. Borshchevsky, *Phys. Rev. B* **55**, 1476 (1997).
- ¹⁴L. Chapon, D. Ravot, and J. C. Tedenac, *J. Alloys Compd.* **282**, 58 (1999).
- ¹⁵G. P. Meisner, D. T. Morelli, S. Hu, J. Yang, and C. Uher, *Phys. Rev. Lett.* **80**, 3551 (1998).
- ¹⁶G. S. Nolas, J. L. Cohn, and G. A. Slack, *Phys. Rev. B* **58**, 164 (1998).
- ¹⁷X. F. Tang *et al.*, *J. Mater. Res.* **16**, 3343 (2001).
- ¹⁸X. Tang, L. Chen, T. Goto, and T. Hirai, *J. Mater. Res.* **16**, 837 (2001).
- ¹⁹L. Chen, Proceedings of the 21st International Conference on Thermoelectrics, Long Beach, California, USA, 25–29 August 2002 (IEEE, Piscataway), p. 42.
- ²⁰D. Bérardan, C. Godart, E. Alleno, S. Berger, and E. Bauer, *J. Alloys Compd.* **351**, 18 (2003).
- ²¹D. Bérardan, E. Alleno, C. Godart, M. Puyet, B. Lenoir, A. Dauscher, D. Ravot, and E. Bauer, Proceedings of the 22nd International Conference on Thermoelectrics ICT2003, La Grand Motte, France, August 2003 (IEEE, Piscataway), p. 56.
- ²²D. Bérardan, E. Alleno, C. Godart, O. Rouleau, and J. Rodriguez-Carvajal, *Mater. Res. Bull.* **40**, 537 (2005).
- ²³H. Anno, J. Nagao, and K. Matsubara, Proceedings of the 21st International Conference on Thermoelectrics, Long Beach, California, USA, 25–29 August 2002 (IEEE, Piscataway), p. 56.
- ²⁴N. R. Dilley *et al.*, *Phys. Rev. B* **61**, 4608 (2000).
- ²⁵N. R. Dilley, E. J. Freeman, E. D. Bauer, and M. B. Maple, *Phys. Rev. B* **58**, 6287 (1998).
- ²⁶E. Matsuoka, K. Hayashi, A. Ikeda, T. Takabatake, and M. Matsumura, *J. Phys. Soc. Jpn.* **74**, 1382 (2005).
- ²⁷D. A. Gajewski *et al.*, *J. Phys.: Condens. Matter* **10**, 6973 (1998).
- ²⁸V. L. Kuznetsov and D. M. Rowe, *J. Phys.: Condens. Matter* **12**, 7915 (2000).
- ²⁹X. F. Tang, L. D. Chen, T. Goto, T. Hirai, and R. Z. Yuan, *J. Mater. Sci.* **36**, 5435 (2001).
- ³⁰M. Lasalle, I. Lefebvre-Devos, X. Wallart, J. Olivier-Fourcade, L. Monconduit, and J. C. Jumas, Proceedings of the 19th International Conference on Thermoelectrics, Cardiff, Wales, UK, 20–24 August 2000 (Babrow Press, UK), p. 98.